THE JOURNAL OF PHYSICAL CHEMISTRY C

Article

pubs.acs.org/JPCC

Ions Transport and Adsorption Mechanisms in Porous Electrodes During Capacitive-Mixing Double Layer Expansion (CDLE)

Raúl A. Rica,* Doriano Brogioli, Roberto Ziano, Domenico Salerno, and Francesco Mantegazza

Dipartimento di Medicina Sperimentale, Universita' di Milano-Bicocca, Via Cadore 48, 20052, Monza, Italy

ABSTRACT: A model of the electro-diffusion of ions in porous electrodes is applied to analyze the dynamics of capacitive-mixing extraction of energy from salinity gradients with carbon porous electrodes. The complex time-evolution of the cell voltage observed in experiments is satisfactorily described. The asymmetry on the duration of the solution-change steps performed in open circuit is found to be due to the nonlinear voltage−concentration relationship of the electric double layers and to a current that redistributes the counterions along the depth of the electrode leading to nonuniform charge and salt adsorption. The validated model is an essential tool for the design and optimization of renewable energy extraction by this technique.

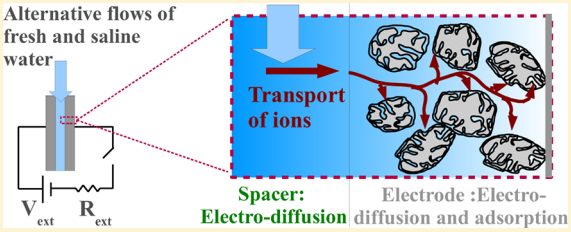

INTRODUCTION

The recently proposed "capacitive mixing" (CAPMIX) methods to extract energy from salinity gradients[1] are attaining great interest, as they are a very promising strategy to extract efficiently renewable energy where the mixing of solutions of different salt concentration takes place naturally, such as at the mouths of rivers in the seas or oceans. The first of such techniques to be proposed was the so-called "capacitive energy extraction based on double layer expansion" (CDLE),[2,3] which prompted the development of similar approaches. Among the CAPMIX techniques, the "capacitive energy extraction based on Donnan potential" (CDP) is included,[4,5] which incorporates ion-selective membranes into the capacitive cell. Other methods use ion-selective nanopores to induce current between reservoirs with different salt concentration,[6] or selective interactions of their electrodes with the ions in solution, called mixing entropy batteries.[7] Altogether, these techniques constitute the field of so-called "blue energy", or salinity-gradient energy.

The origin of such renewable energy release is due to the increase in entropy that occurs upon mixing two electrolyte solutions of different salt concentration, a process that spontaneously takes place at the mouths of rivers: ∼2.2 kJ are released per liter of river water that is poured into the sea.[8,9] The efficiency and economic competitiveness of previous attempts to tap this renewable source of energy have been hindered by technological difficulties and elevate costs of components, all of them requiring the use of extensive areas of perm-selective membranes.[10,11]

CDLE is based on the dependence on salt concentration of the differential capacitance of the electric double layer (EDL), the nonuniform distribution of like-charged and oppositely charged ions (co-ions and counterions, respectively) that develops close to a charged surface in order to keep electroneutrality. Direct generation of energy with inexpensive materials (porous carbon supercapacitors[12,13]) is attained in CDLE by changing the solution where a pair of charged electrodes are immersed by another solution with lower salinity. If the stored charge is kept constant during the solution change, that is, in open circuit configuration, the capacitance of the EDL decreases, leading to an increase in the cell voltage and of the stored electrostatic energy. A common feature of CAPMIX technologies is the fact that the transport of ions inside the porous electrodes plays a key role in their performance. Therefore, the optimization requires not only the development of accurate EDLs models describing their charge−voltage relationship[14,15] but also the consideration of the transport of ions inside the porous matrix.[16,17]

In this work, we apply a 1D theory of the electro-diffusion of ions in porous electrodes developed by Biesheuvel and Bazant[16] to analyze the rich physical phenomena observed in experiments with a CDLE prototype cell, which includes the transport, adsorption, and desorption of ions in the porous electrodes. Although some improvements of the model (like faradaic reactions, steric effects, and multi-ions effects[17−19] or 2D modeling) must be included for a quantitative analysis, the used 1D theory demonstrates to be accurate enough to identify the different time scales and transport mechanisms during the CDLE cycle, whose understanding is essential to maximize the power output. The 1D approach has been successfully applied in several previous works[20−22] devoted to the description of "capacitive deionization" (CDI), a technique that, inversely to CDLE, consumes energy for removing ions from salty water by storing them in the EDLs of a pair of porous carbon electrodes.[23−25] In fact, it has been recently shown that CDI and CDLE are intrinsically connected.[26]

Received: June 18, 2012
Revised: July 20, 2012
Published: July 24, 2012

 © 2012 American Chemical Society dx.doi.org/10.1021/jp3059849 | J. Phys. Chem. C 2012, 116, 16934−16938

METHODS

The full CDLE cycle is as follows[2] (see Figure 1). The CAPMIX cell is submerged in a electrolyte solution of

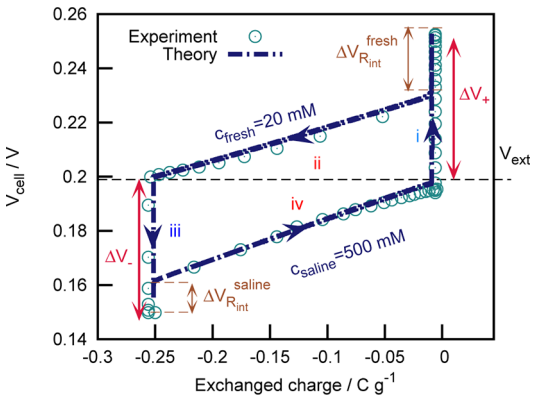

Figure 1. Measured (symbols) and simulated (line) CAPMIX cycle in the cell voltage-exchanged charge per gram of electrode space. Latin numbers refer to the four different steps of a CAPMIX cycle, as numbered in the main text. The exchanged charge is the integral of the current (I_{ext}) through the external load in the charge and discharge steps, its zero value corresponding to the initial state. Characteristics of prototype cell: two parallel plate, Norit S30 carbon (BET area: 1650 m^2/g) electrodes; geometric area of electrodes A = 1.5 × 1.5 cm^2; electrode nominal thickness L_e = 100 μm; distance between electrodes δ = 1 mm; external loads $R_{ext,fresh}$ = 25Ω and $R_{ext,saline}$ = 5Ω. $D = D_{mA} = D_{NaCl}$. Free parameters of the simulation: $C_{St,vol}$ = 0.06GF/m^3; p_{mi} = 0.3; p_{mA} = 0.4; L_e = 85 μm.

concentration C_{saline} (500 mM NaCl in this work) and then externally charged until a voltage difference $V_{cell} = V_{ext}$ is established between its two electrodes. With this initial state, the electrochemical cell is operated performing a four-step cycle: (i) Change the solution from C_{saline} to another with lower salt content C_{fresh} (20 mM NaCl in this work) at constant stored charge (i.e., in open circuit). The cell voltage spontaneously increases to $V_{cell} = V_{ext} + \Delta V_+$. (ii) Discharge the electrodes through an external load ($R_{ext,fresh}$) to $V_{cell} = V_{ext}$. (iii) Change the salt content of the solution from C_{fresh} to C_{saline} at constant stored charge. The cell voltage spontaneously decreases to $V_{cell} = V_{ext} - \Delta V_-$. (iv) Charge the electrodes through an external load ($R_{ext,saline}$) to $V_{cell} = V_{ext}$.

The energy extracted by this cycle is the area enclosed in the curve of Figure 1, whose theoretical quantification requires the aforementioned charge−voltage relationship. Classical descriptions of the EDL are not valid inside the micropores of activated carbon particles, which have a size comparable to the EDL thickness and even to that of hydrated ions, leading to EDLs overlap and other complications, such as the observed very large values of the capacitance.[27−30] In this work, we use the recent "modified Donnan" (mD) model,[17,25] described below, which is valid in the limit of EDL thickness much larger than the characteristic size of micropores.

The cell voltage is given by a contribution due to the EDLs on each electrode ΔV_{EDL}, which we assume to be symmetric, and by a contribution due to the internal resistance $\Delta V_{R_{int}}$. Therefore, we express the cell voltage as $V_{cell} = 2\Delta V_{EDL} - \Delta V_{R_{int}}$. The latter term is calculated from the conductivity of the solution in the spacer channel and inside the macropores, and the current through the cell, whereas ΔV_{EDL} is given by the EDL model. It is common to distinguish between two regions in the EDL, which are called the diffuse and the Stern layers[31]

$$\Delta V_{EDL} = (\Delta\phi_D + \Delta\phi_{St})V_T \quad (1)$$

where $\Delta\phi_D = V_D/V_T$ and $\Delta\phi_{St} = V_{St}/V_T$ are the normalized voltages along the diffuse and the Stern layers, respectively. Here $V_T = k_BT/e$ is the thermal voltage, k_B is the Boltzmann constant, T is absolute temperature, and e is the electron charge.

The electrodes are made of activated carbon particles with a characteristic size of the order of the micrometer, which are assembled and sintered together. These particles are themselves porous, presenting a very large specific surface inside the small micropores (≤2 nm). Therefore, the free space between different carbon particles filled with electroneutral solution (with concentration $C_{i,mA} = C_{mA}$, where $i = \pm$ applies to cations and anions, respectively) constitutes a macroporosity that serves as a path for salt and charge transport, whereas the micropores store ionic charge in their EDLs. The micro- and macro-porosities p_{mi} and p_{mA} are defined as the volume fraction occupied by micro- and macro-pores to the total electrode volume, respectively.

The mD model assumes a constant electric potential in the diffuse layer inside the micropores and a charge-free Stern layer, accounting for the minimum approach of ions to the surface. In the case of a monovalent, binary electrolyte, the concentration of cations and anions in the diffuse part of the EDLs inside the micropores is also constant and given by $C_{\pm,mi} = C_{mA}\exp(\mp\Delta\phi_D)$. To simplify matters, we introduce some dimensionless quantities in what follows. The concentrations are normalized by C_{saline}, and thus $c_{\pm,mi} = C_{\pm,mi}/C_{saline}$ and $c_{mA} = C_{mA}/C_{saline}$. The dimensionless charge density in the diffuse part of the EDLs in the micropores $q_{mi} = 1/2(c_{+,mi} - c_{-,mi})$ is related to $\Delta\phi_D$ and $\Delta\phi_{St}$ through

$$q_{mi} = -c_{mA}\sinh\Delta\phi_D = -\frac{\Delta\phi_{St}}{\delta_{mD}} \quad (2)$$

where $\delta_{mD} = (2eC_{saline})/(V_TC_{St,vol})$ and $C_{St,vol}$ is a volumetric Stern capacitance. During electrode charging, salt adsorption takes place together with charge adsorption because counter-ions attraction exceeds the expulsion of co-ions from the EDLs when the condition $V_D \ll V_T$ is not verified.[32] This is characterized by the concentration of ions of either type inside the micropores, $w_{mi} = 1/2(c_{+,mi} + c_{-,mi}) = c_{mA}\cosh\Delta\phi_D$.

Although eqs 1 and 2 suffice to simulate a CAPMIX cycle like the one shown in Figure 1, they do not inform about the dynamics during the cycle. For this aim, the electro-diffusion of ions inside the porous electrodes has to be taken into account. It can be described by 1D charge and mass balances in the direction $\hat{x}$ perpendicular to the electrodes and to the flow in the spacer channel. We distinguish between two regions (see Figure 2): the stagnant diffusion layer (SDL) ($-L_{SDL} < x < 0$), that is, a transition region out of the electrode matrix where the electric potential and the salt concentration change from their values in the bulk to those inside the electrode,[16,33,34] and the electrode itself ($0 < x < L_e$), where charge and salt adsorption have to be taken into account. This treatment leads to the Ohm's law and the diffusion equation for the ions in the SDL, out of the electrode matrix[16]

$$i_{SDL} = -2Dc_{SDL}\frac{\partial\phi_{SDL}}{\partial x} \quad (3)$$

dx.doi.org/10.1021/jp3059849 | J. Phys. Chem. C 2012, 116, 16934−16938

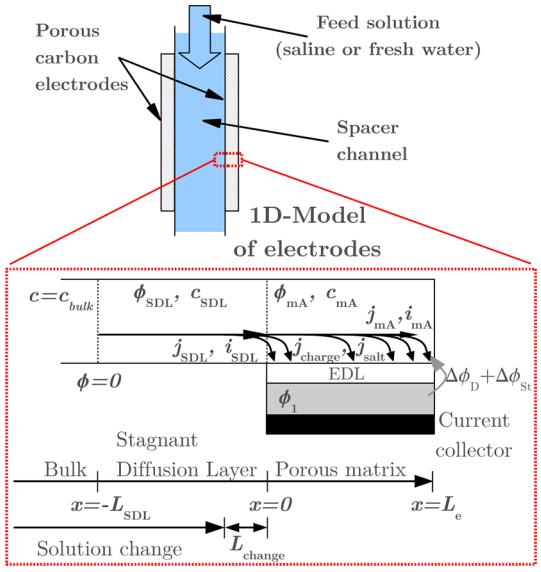

Figure 2. One-dimensional model of electro-diffusion of ions in porous electrodes applied to CAPMIX. The uniform rates of charge ($i_{SDL}(t)$) and neutral salt ($j_{SDL}(t)$) transport in the stagnant diffusion layer (SDL) due to gradients of salt concentration and electric potential are modified inside the porous matrix due to adsorption of both charge ($j_{charge}(x,t)$) and salt ($j_{salt}(x,t)$) into the EDLs that form at the solid−liquid interface, leading to position- (and time-) dependent quantities $i_{mA}(x,t)$ and $j_{mA}(x,t)$. The local values of electric potential ($\phi(x,t)$) and salt concentration ($c(x,t)$) determine, together with the adsorbed charge in the EDLs, the (unique) electrode potential through appropriate EDL models. At the beginning of the open circuit steps, the solution in the bulk and in part of the SDL is substituted. The part of the SDL that is not changed instantaneously is determined by the length L_{change}. C_{bulk} is either C_{saline} or C_{fresh}.

$$\frac{\partial c_{SDL}}{\partial t} = D\frac{\partial^2 c_{SDL}}{\partial x^2} \tag{4}$$

where $i_{SDL} = I_{SDL}/C_{saline}V_T$ is the dimensionless current density in the SDL (note that it is constant along the whole SDL) and D is the bulk diffusion coefficient.

Inside the porous matrix, these equations have to be modified to include the adsorption rates of charge ($j_{charge} = \partial q_{mi}/\partial t$) and salt ($j_{salt} = \partial w_{mi}/\partial t$) into the EDLs[16]

$$\frac{\partial i_{mA}}{\partial x} = -\frac{p_{mi}}{p_{mA}}\left(\frac{\partial q_{mi}}{\partial t}\right) \tag{5}$$

$$\frac{\partial c_{mA}}{\partial t} = D_{mA}\frac{\partial^2 c_{mA}}{\partial x^2} - \frac{p_{mi}}{p_{mA}}\left(\frac{\partial w_{mi}}{\partial t}\right) \tag{6}$$

where $i_{mA} = -2D_{mA}c_{mA}(\partial\phi_{mA}/\partial x)$ and D_{mA} are the dimensionless current density and the diffusion coefficient in the porous matrix, respectively. D_{mA} is different from its bulk value D to account for the tortuosity. The boundary conditions at the macroscopic electrode−solution interface ($x = 0$) require the continuity of the fluxes of every ionic specie, salt concentration, and electric potential. Furthermore, the electric current is constant along all of the circuit (the CAPMIX cell and the external circuit, composed of the external source and the load). The salinity change steps, performed in open circuit ($I_{ext} = 0$), are done by instantaneously substituting the solution in the spacer, leaving unchanged the solution in a layer close to the electrode of thickness L_{change}. In this work, we arbitrarily set its value to $L_{change} = 20\ \mu$m. A more detailed description of the model and its solution can be found in the original work.[16] In the present work, we numerically solve the coupled set of eqs 1−6 together with the specified boundary conditions.

RESULTS AND DISCUSSION

Figure 3 illustrates the nontrivial dynamics, followed by V_{cell} during the operation of a CDLE cell. As we can see, after the four-step cycle, the cell comes back to its initial state demonstrating the feasibility of the technique. Together with the measured cycle, we have also plotted in Figure 3 the results of the discussed model, and a very good agreement between measurements and the numerical solution of eqs 1−6 is found.

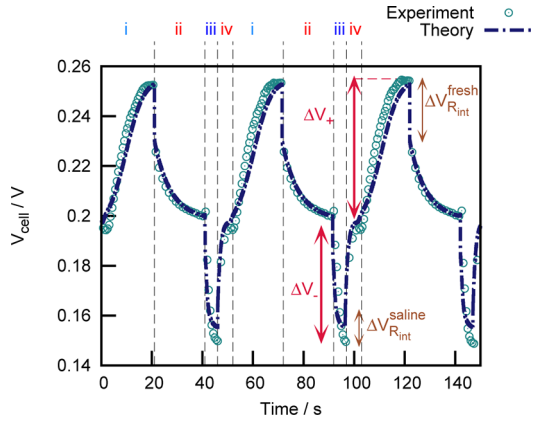

Figure 3. Comparison between the measured (symbols) and simulated (line) time evolution of V_{cell} along three consecutive CAPMIX cycles such as the one of Figure 1. In the open circuit steps (i and iii), the new solution flows for 5 s.

Whereas the charge and discharge steps have been previously analyzed,[16] the open circuit steps present new phenomenology, with transport mechanisms with different time scales others than salt diffusion. When the solution is changed from saline to fresh water, salt diffuses from the highly concentrated macropores toward the fresh solution, thus establishing a concentration gradient inside the porous matrix and the bulk (quite sharp at short times after the switching, $\tau \simeq L_{change}^2/D \leq 1$ s, smoothing out on larger time scales). After the fresh-to-saline change, diffusion takes place from the spacer to the macropores. As already observed,[2,3] the time evolution of the cell voltage upon solution change is asymmetric (see Figure 3), as the time needed to stabilize the voltage rise (switch from saline water to fresh water) is much longer than the characteristic fall time (fresh to saline) and also from the characteristic time of the diffusion inside the macropores of the electrode. Here we show that this behavior is mainly due to the highly nonlinear voltage−concentration relation, as shown in Figure 4: when the concentration is above 200 mM, the voltage changes very little with concentration, whereas below that value the dependence is very strong.

Indeed Figure 4 shows the position-dependent path, followed by the cell in the voltage−concentration space. Remarkably, the highest salt concentration $C_{saline} = 500$ mM is not reached at any point inside the porous matrix. This is due to the nonlinearity of the voltage−concentration dependence, which makes the cell voltage saturate at about $C_{mA} = 300$ mM. As the cell is operated in view of the cell voltage, the next step

dx.doi.org/10.1021/jp3059849 | J. Phys. Chem. C 2012, 116, 16934−16938

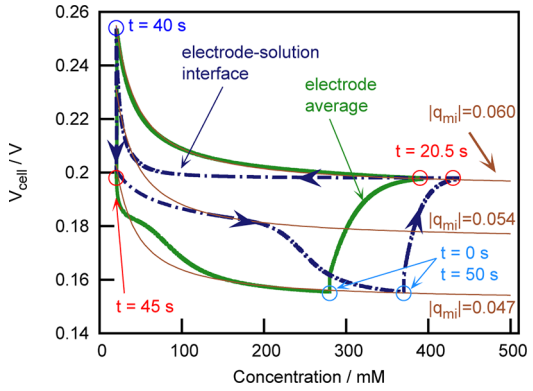

Figure 4. Thin solid lines, bottom to top: cell voltage versus salt concentration relations for $|q_{mi}|$ = 0.047, 0.054, and 0.06. Dashed-dotted and thick solid lines: simulated CAPMIX cycle in Figure 1, showing the evolution of the cell voltage with the salt concentration at the macroscopic electrode−solution interface (which determines the position x = 0) and average concentration in the electrode, respectively. Circles locate the initial state of each step, starting at the indicated times.

is taken when it reaches a plateau, before the salt concentration gradient is canceled.

Of outermost importance is the evolution of V_{cell} with the concentration in the solution at the macroscopic electrode-spacer interface (x = 0), as it directly relates $\Delta V_{EDL}(x = 0)$ to the electrode potential through the voltage drop in the spacer ΔV_{Rint}, without contributions from the resistivity of macropores. In this case, we see that in the saline-to-fresh solution open-circuit step, the concentration at x = 0 changes from about 400 to 100 mM concentration without any effect on V_{cell}. This happens because V_{cell} does not follow any constant-charge path in the open circuit steps but a more complex one. Within the short time scale where a salinity gradient is established after changing the solution, gradients of charge and salt adsorption also appear, as the ionic charge in the micropores is redistributed along the electrode, as shown in Figure 5. A current inside the electrode transports counterions from the surface micropores toward those deeper in the electrode, although the external current (equal to that flowing from one electrode to the other through the spacer) is zero. Of course,

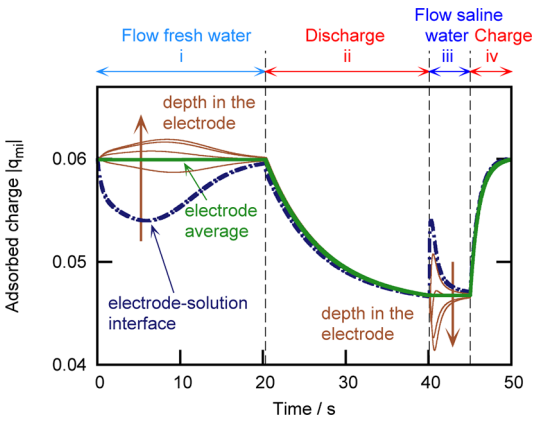

Figure 5. Time evolution over one of the CAPMIX cycles in Figure 3 of the adsorbed charge density at different depths in the electrode. Dashed-dotted line: $|q_{mi}|$ at the macroscopic electrode−solution interface, which determines the position x = 0. Thin, solid lines, in the order determined by the arrow: x = 0.25 L_e, 0.5 L_e, 0.75 L_e, L_e.

the total current on each electrode is conserved, as confirmed by the constant value of the average charge in the electrode during the open-circuit steps.

The redistribution of counterions significantly influences the evolution of V_{cell} with salt concentration. Such mechanism is responsible of the transitions in the path, followed by the cell in the $V_{cell} - c(x = 0)$ space shown in Figure 4 from the $|q_{mi}|$ = 0.06 curve to the $|q_{mi}|$ = 0.054 one in the saline-to-fresh step and of that between $|q_{mi}|$ = 0.054 and $|q_{mi}|$ = 0.047 in the fresh-to-saline one.

It is interesting to note that this redistribution mechanism is also expected to take place along the length of the electrodes due to the presence of a concentration gradient in this direction, whereas the solutions are exchanged. Because of the short electrodes used in our present experiments (1.5 cm), we could neglect this effect in our treatment, as the solution is effectively changed in a couple of seconds, much faster than the characteristic times of voltage stabilization and charge redistribution. Therefore, a 2D analysis of the CAPMIX cycle would be desirable. However, as previously mentioned, the 1D model suffices to explain the experiments performed in the present contribution.

Finally, we must come back to the assumption of EDL overlap inside micropores. Although it is very likely to take place when the concentration of the solution in the cell is 20 mM, such overlap is expected to be weaker when the concentration is 500 mM. Therefore, the model should include the transport of ions along the micropores, at least in the high salinity steps. Such an inclusion would considerably complicate the theoretical analysis and would require a larger computational effort. However, we can justify our simplification on two points. On the one hand, it is well known that the actual length over which EDLs extend is larger than that given by the Debye length, covering distances to the surface several times larger than this characteristic size. Furthermore, it has been recently shown that steric effects increase the value of the Debye length.[18,28] On the other hand, the diffusion inside the micropores in the absence of EDL overlap (seawater) would slow down the dynamics, leading to a more similar characteristic times of the fresh-to-saline and the saline-to-fresh solution change steps. Therefore, although its inclusion is certainly important, it can be neglected in the present study aiming at the identification of the mechanisms responsible of the observed asymmetry.

■ CONCLUSIONS

In summary, we have shown that the used model of the electrodiffusion of ions in porous electrodes is able to describe fairly well the full cyclic process of energy harvesting from salinity gradients with CDLE. The complex evolution of the cell potential observed in experiments has been explained, taking into account the adsorption and desorption of charge and salt into the micropores, the nonlinearity of the charge−voltage relations of the EDLs, and the transport of salt and charge in the electro-neutral macropores of the carbon electrodes. Altogether, these mechanisms lead to nonuniform charge and salt adsorption in the electrodes, considerably affecting the performance of the CAPMIX cell. The model thus validated is a key tool for the optimization of the CDLE technique.

■ AUTHOR INFORMATION

Corresponding Author

*E-mail: rul@ugr.es.

dx.doi.org/10.1021/jp3059849 | J. Phys. Chem. C 2012, 116, 16934−16938

Notes

The authors declare no competing financial interest.

■ ACKNOWLEDGMENTS

The research leading to these results received funding from the European Union Seventh Framework Programme (FP7/2007-2013) under agreement no. 256868. R.A.R. acknowledges support from Regione Lombardia (Accordo per lo sviluppo del capitale umano nel sistema universitario lombardo). F.M. and D.S. acknowledge support of Cariplo Foundation Materiali avanzati -2011, Project 2011-0336.

■ REFERENCES

(1) Bijmans, M.; Burheim, O.; Bryjak, M.; Delgado, A.; Hack, P.; Mantegazza, F.; Tenisson, S.; Hamelers, H. *Energy Procedia* **2012**, *20*, 108−115.
(2) Brogioli, D. *Phys. Rev. Lett.* **2009**, *103*, 058501.
(3) Brogioli, D.; Zhao, R.; Biesheuvel, P. M. *Energy Environ. Sci.* **2011**, *4*, 772−777.
(4) Sales, B. B.; Saakes, M.; Post, J. W.; Buisman, C. J. N.; Biesheuvel, P. M.; Hamelers, H. V. M *Environ. Sci. Technol.* **2010**, *44*, 5661−5665.
(5) Liu, F.; Schaetzle, O.; Sales, B. B.; Saakes, M.; Buisman, C.; Hamelers, H. V. M. *Energy Environ. Sci.* **2012**, in press. DOI: 10.1039/C2EE21548A.
(6) Guo, W.; Cao, L.; Xia, J.; Nie, F.-Q.; Ma, W.; Xue, J.; Song, Y.; Zhu, D.; Wang, Y.; Jiang, L. *Adv. Funct. Mater.* **2010**, *20*, 1339−1344.
(7) La Mantia, F.; Pasta, M.; Deshazer, H. D.; Logan, B. E.; Cui, Y. *Nano Lett.* **2011**, *11*, 1810−1813.
(8) Pattle, R. E. *Nature* **1954**, *174*, 660.
(9) Norman, R. S. *Science* **1974**, *186*, 350−352.
(10) Post, J. W.; Veerman, J.; Hamelers, H. V. M; Euverink, G. J. W.; Metz, S. J.; Nymeijer, K.; Buisman, C. J. N. *J. Membr. Sci.* **2007**, *288*, 218−230.
(11) Yip, N. Y.; Elimelech, M. *Environ. Sci. Technol.* **2011**, *45*, 10273−10282.
(12) Simon, P.; Gogotsi, Y. *Nat. Mater.* **2008**, *7*, 845−854.
(13) Candelaria, S. L.; Shao, Y.; Zhou, W.; Li, X.; Xiao, J.; Zhang, J.-G.; Wang, Y.; Liu, J.; Li, J.; Cao, G. *Nano Energy* **2012**, *1*, 195−220.
(14) Carrique, F.; Arroyo, F. J.; Delgado, A. V. *J. Colloid Interface Sci.* **2002**, *252*, 126−137.
(15) Boon, N.; Van Roij, R. *Mol. Phys.* **2011**, *109*, 1229−1241.
(16) Biesheuvel, P. M.; Bazant, M. Z. *Phys. Rev. E* **2010**, *81*, 031502.
(17) Biesheuvel, P. M.; Fu, Y.; Bazant, M. Z. *Phys. Rev. E* **2011**, *83*, 061507.
(18) Bazant, M. Z.; Kilic, M. S.; Storey, B. D.; Ajdari, A. *Adv. Colloid Interface Sci.* **2009**, *152*, 48−88.
(19) Biesheuvel, P.; Fu, Y.; Bazant, M. *Russ. J. Electrochem.* **2012**, *48*, 580−592.
(20) Porada, S.; Sales, B. B.; Hamelers, H. V. M; Biesheuvel, P. M. *J. Phys. Chem. Lett.* **2012**, *3*, 1613−1618.
(21) Suss, M. E.; Baumann, T.; Bourcier, B.; Spadaccini, C.; Rose, K. A.; Santiago, J. G.; Stadermann, M. *Energy Environ. Sci.* **2012**, DOI: 10.1039/C2EE21498A.
(22) Zhao, R.; van Soestbergen, M.; Rijnaarts, H.; van der Wal, A.; Bazant, M.; Biesheuvel, P. *J. Colloid Interface Sci.* **2012**, DOI: 10.1016/j.jcis.2012.06.022.
(23) Oren, Y. *Desalination* **2008**, *228*, 10−29.
(24) Biesheuvel, P. M.; van Limpt, B.; van der Wal, A. *J. Phys. Chem. C* **2009**, *113*, 5636−5640.
(25) Biesheuvel, P. M.; Zhao, R.; Porada, S.; van der Wal, A. *J. Colloid Interface Sci.* **2011**, *360*, 239−248.
(26) Rica, R. A.; Ziano, R.; Salerno, D.; Mantegazza, F.; Brogioli, D. *Phys. Rev. Lett.* **2012**, under review.
(27) Chmiola, J.; Yushin, G.; Gogotsi, Y.; Portet, C.; Simon, P.; Taberna, P. L. *Science* **2006**, *313*, 1760−1763.
(28) Das, S.; Chakraborty, S. *Phys. Rev. E* **2011**, *84*, 012501.
(29) Das, S.; Chakraborty, S.; Mitra, S. K. *Phys. Rev. E* **2012**, *85*, 051508.
(30) Merlet, C.; Rotenberg, B.; Madden, P. A.; Taberna, P. L.; Simon, P.; Gogotsi, Y.; Salanne, M. *Nat. Mater.* **2012**, *11*, 306−310.
(31) Lyklema, J. *Fundamentals of Interface and Colloid Science*; Academic: New York, 1995; Vol. *2*.
(32) Bazant, M. Z.; Thornton, K.; Ajdari, A. *Phys. Rev. E* **2004**, *70*, 021506.
(33) Kim, S.; Hoek, E. M. *Desalination* **2005**, *186*, 111−128.
(34) Andersen, M. B.; van Soestbergen, M.; Mani, A.; Bruus, H.; Biesheuvel, P. M.; Bazant, M. Z. *Phys. Rev. Lett.* **2012**, in press.